Institute for Advanced Simulation

Multiscale Modelling of Magnetic Materials: From the Total Energy of the Homogeneous Electron Gas to the Curie Temperature of Ferromagnets

Phivos Mavropoulos

published in

Multiscale Simulation Methods in Molecular Sciences,
J. Grotendorst, N. Attig, S. Blügel, D. Marx (Eds.),
Institute for Advanced Simulation, Forschungszentrum Jülich,
NIC Series, Vol. **42**, ISBN 978-3-9810843-8-2, pp. 271-290, 2009.

http://www.fz-juelich.de/nic-series/volume42

Multiscale Modelling of Magnetic Materials: From the Total Energy of the Homogeneous Electron Gas to the Curie Temperature of Ferromagnets

Phivos Mavropoulos

Institute for Solid State Research and Institute for Advanced Simulation
Forschungszentrum Jülich, 52425 Jülich, Germany
E-mail: Ph.Mavropoulos@fz-juelich.de

A widely used multiscale approach for the calculation of temperature-dependent magnetic properties of materials is presented. The approach is based on density functional theory, which, starting only from fundamental physical constants, provides the ground-state magnetic structure and a reasonable parametrization of the excited-state energies of magnetic systems, usually in terms of the Heisenberg model. Aided by statistical mechanical methods for the solution of the latter, the approach is at the end able to predict to within 10-20% high-temperature, material-specific magnetic properties such as the Curie temperature or the correlation function without the need for any fitting to experimental results.

1 Introduction

The physics of magnetism in materials spans many length scales. Starting from the formation of atomic moments by electron spins on the Ångström scale, it extends through the inter-atomic exchange interaction on the sub-nanometer scale to the formation of magnetic domains and hysteresis phenomena on the mesoscopic and macroscopic scale. In addition, the physics of magnetism spans many energy scales. The moments formation energy can be of the order of a few eV, the inter-atomic exchange of the order of 10-100 meV, elementary spin-wave excitations are of the order of 1-10 meV, while the magnetocrystalline anisotropy energy can be as low as a μeV. An energy-frequency correspondence implies the importance of as many time scales: from characteristic times of femto-seconds, related to the inter-atomic electron hopping and the atomic moments, through pico-seconds, related to the magnonic excitations, to seconds, hours or years related to the stability of a macroscopic magnetic configuration, e.g. defining a bit of information on a hard disc drive.

Clearly, a unified description of all these scales on the same footing is impossible. While many-body quantum mechanical calculations are necessary for the understanding of the small length scale phenomena, simple, possibly classical models have to suffice for the large scale. In this situation, multiscale modelling can provide a description on all scales, without adjusting parameters to experiment, but rather using results from one scale as input parameters to the model of the next scale. The scope of this manuscript is the presentation of such an approach, called here the Multiscale Programme, which is widely applied in present day calculations of magnetic material properties.

The manuscript is meant to serve as an introduction to the subject, not as a review. The list of references is definitely incomplete, reflecting only some suggested further reading. Finally, it should be noted that there are other multiscale concepts in magnetism, mainly in

the direction of micromagnetics and time evolution of the magnetization, as mentioned in Sec. 7.3. This type of multiscale modelling is an important field, however its description is beyond the scope of the present manuscript.

2 Outline of the Multiscale Programme

The outline of the Multiscale Programme can be summarized by the following steps, which will be explained in more detail in the next sections:

1. Calculation of the exchange-correlation energy of the electron gas, $E_{\rm xc}[\rho]$, as a functional of the electron density $\rho(\vec{r})$ by quantum Monte Carlo calculations and/or many-body theory.

2. Proper (approximate) parametrization of $E_{\rm xc}[\rho]$, usually in terms of ρ and $\nabla\rho$.

3. Use of $E_{\rm xc}[\rho]$ in density functional calculations for the unconstrained ground-state properties of a magnetic material (in particular, ground state atomic magnetic moments $\vec{M}_n$ and total energy $E^0_{\rm tot}$).

4. Use of $E_{\rm xc}[\rho]$ in *constrained* density functional calculations for the ground-state properties of a magnetic material under the influence an external, position-dependent magnetic field that forces a rotation of the magnetic moments $\{\vec{M}_n\}$, resulting in a total energy $E^{\rm constr}_{\rm tot}(\{\vec{M}_n\})$.

5. The adiabatic hypothesis: assumption that the time-scale of low-lying magnetic excitations is much longer than the one of inter-site electron hopping, so that $E^{\rm constr}_{\rm tot}(\{\vec{M}_n\})$ is a good approximation to the total energy of the excited state.

6. Correspondence to the Heisenberg hamiltonian under the assumption that $\Delta E(\{\vec{M}_n\}) := E^{\rm constr}_{\rm tot}(\{\vec{M}_n\}) - E^0_{\rm tot} \simeq -\frac{1}{2}\sum J_{nn'}\,\vec{M}_n\cdot\vec{M}_{n'} + {\rm const.}$

7. Solution of the Heisenberg hamiltonian $H = -\frac{1}{2}\sum_{nn'} J_{nn'}\,\vec{M}_n\cdot\vec{M}_{n'}$, e.g. for the Curie temperature, via a Monte Carlo method.

Steps 3 and 6 are connecting different models to each other.

3 Principles of Density Functional Theory

The most widely used theory for quantitative predictions with no adjustable parameters in condensed matter physics is density functional theory (DFT). “No adjustable parameters” means that, in principle, only fundamental constants are taken from experiment: the electron charge, Planck’s constant, and the speed of light in vacuum. Given these (and the types of atoms that are present in the material of interest), DFT allows to calculate ground-state properties of materials, such as the total energy, ground-state lattice structure, charge density, magnetization, etc. Naturally, since in practice the method relies on approximations to the exchange and correlation energy of the many-body electron system, the results are not always quantitatively or even qualitatively correct.

3.1 The Hohenberg-Kohn theorems and the Kohn-Sham ansatz

Density functional theory relies on the theorems of Hohenberg and Kohn.[1] Loosely put, these state that the ground-state wave function of a many-electron gas (under the influence of an external potential) is uniquely defined by the ground-state density (ground-state wavefunctions and densities are in one-to-one correspondence), and that an energy functional of the density exists that is stationary at the ground-state density giving the ground-state energy. Thus a variational scheme (introduced by Kohn and Sham[2]) allows for minimization of the energy functional in terms of the density, yielding the ground-state density and energy. Within the Kohn-Sham scheme[2] for this minimization, an auxiliary system of non-interacting (with each other) electrons is introduced, obeying a Schrödinger-like equation in an effective potential $V_{\rm eff}$. The effective potential includes the Hartree potential and exchange-correlation effects which depend explicitly on the density, as well as the "external" potential of the atomic nuclei (external in the sense that it does not arise from the electron gas). The Schrödinger-like equation must then be solved self-consistently so that the density is reproduced by the auxiliary electron system. In order for the scheme to work, a separation of the total energy functional is done:

$$E_{\rm DFT}[\rho] = T_{\rm n.i.}[\rho] + E_{\rm ext}[\rho] + E_{\rm H}[\rho] + E_{\rm xc}[\rho]. \tag{1}$$

Here, $T_{\rm n.i.}$ is the kinetic energy of the auxiliary non-interacting electrons, $E_{\rm ext} = \int d^3r\, \rho(\vec{r})\, V_{\rm ext}(\vec{r})$ is the energy due to the external potential (e.g., atomic nuclei), $E_{\rm H} = -e^2 \frac{1}{2} \int d^3r \int d^3r' \rho(\vec{r})\rho(\vec{r}')/|\vec{r}-\vec{r}'|$ is the Hartree energy, and $E_{\rm xc}$ is "all that remains", i.e., the exchange and correlation energy. All but the latter can be calculated with arbitrary precision, while $E_{\rm xc}$ requires some (uncontrolled) approximation which also determines the accuracy of the method.

In practice, DFT calculations rely on a local density approximation (LDA) to the exchange-correlation energy. This means that $E_{\rm xc}[\rho]$ is approximated by $E_{\rm xc}^{\rm LDA}[\rho] = \int d^3r\, \varepsilon_{\rm xc}^{\rm hom}(\rho(\vec{r}))\, \rho(\vec{r})$, where $\varepsilon_{\rm xc}^{\rm hom}(\rho)$ is the exchange-correlation energy per particle for a homogeneous electron gas of density ρ. In case of spin-polarized calculations, the spin density $\vec{m}(\vec{r})$ must be included, and ρ is replaced by the density matrix $\boldsymbol{\rho}(\vec{r}) = \rho(\vec{r})\,\mathbf{1} + \vec{\boldsymbol{\sigma}} \cdot \vec{m}(\vec{r})$ ($\vec{\boldsymbol{\sigma}}$ are the Pauli matrices and $\mathbf{1}$ the unit matrix); then we have the local spin density approximation (LSDA). Gradient corrections, taking into account also $\nabla\boldsymbol{\rho}$, lead to the also widely used generalized gradient approximation (GGA).

Henceforth we will denote by $\rho_{\rm min}$, $\vec{m}_{\rm min}$, and $\boldsymbol{\rho}_{\rm min}$ the density, spin density, and density matrix that yield the minimum of energy functionals (either within DFT or constrained DFT, to be discussed in Sec. 5.1). These can be found by application of the Rayleigh-Ritz variational principle to eq. (1) which leads to the Schrödinger-like equation:

$$\left(-\frac{\hbar^2}{2m}\nabla^2 + V_{\rm eff}(\vec{r}) + \vec{\boldsymbol{\sigma}} \cdot \vec{B}_{\rm eff}(\vec{r}) - E_i \right) \begin{pmatrix} \psi_{i\uparrow}(\vec{r}) \\ \psi_{i\downarrow}(\vec{r}) \end{pmatrix} = 0. \tag{2}$$

This is the first of the Kohn-Sham equations for the one-particle eigenfunctions $\psi_{\uparrow,\downarrow}(\vec{r}; E)$ (dependent on spin 'up' ($\uparrow$) or 'down' ($\downarrow$) with respect to a local magnetization direction $\hat{\mu}(\vec{r})$ along $\vec{B}_{\rm eff}(\vec{r})$) and eigenenergies E_i of the auxiliary non-interacting-electron system. The set of Kohn-Sham equations is completed by the expressions for charge and spin

density,

$$\rho(\vec{r}) = \sum_{E_i \leq E_\mathrm{F}} \left(|\psi_{i\uparrow}(\vec{r})|^2 + |\psi_{i\downarrow}(\vec{r})|^2 \right) \tag{3}$$

$$\vec{m}(\vec{r}) = \hat{\mu}(\vec{r}) \sum_{E_i \leq E_\mathrm{F}} \left(|\psi_{i\uparrow}(\vec{r})|^2 - |\psi_{i\downarrow}(\vec{r})|^2 \right), \tag{4}$$

and the requirement for charge conservation that determines the Fermi level E_F,

$$N = \int d^3r \rho(\vec{r}) = \int d^3r \sum_{E_i \leq E_\mathrm{F}} \left(|\psi_{i\uparrow}(\vec{r})|^2 + |\psi_{i\downarrow}(\vec{r})|^2 \right). \tag{5}$$

Expressions (2-5) form the set of non-linear equations to be solved self-consistently in any DFT calculation. The effective potential $V_\mathrm{eff}(\vec{r})$ and magnetic field $\vec{B}_\mathrm{eff}(\vec{r})$ follow from functional derivation of the total energy terms $E_\mathrm{ext}[\rho]$, $E_\mathrm{H}[\rho]$, and $E_\mathrm{xc}[\boldsymbol{\rho}]$ with respect to $\rho(\vec{r})$ and $\vec{m}(\vec{r})$. At the end of the self-consistency procedure one obtains the ground-state energy $E^0_\mathrm{tot} = E_\mathrm{DFT}[\boldsymbol{\rho}_\mathrm{min}]$.

In terms of the single-particle energies E_i, the total energy (1) can be split into the "single-particle" part E_sp and a "double-counting" E_dc part as

$$E_\mathrm{DFT} = E_\mathrm{sp} + E_\mathrm{dc} \tag{6}$$

with

$$E_\mathrm{sp} = \sum_{E_i \leq E_\mathrm{F}} E_i \tag{7}$$

$$E_\mathrm{dc} = -\int d^3r \left(\rho(\vec{r})\, V_\mathrm{eff}(\vec{r}) + \vec{m}(\vec{r}) \cdot \vec{B}_\mathrm{eff}(\vec{r}) \right) + E_\mathrm{H}[\rho] + E_\mathrm{ext}[\rho] + E_\mathrm{xc}[\boldsymbol{\rho}]. \tag{8}$$

3.2 Exchange-correlation energy of the homogeneous electron gas

The total energy of the homogeneous electron gas can be split, following the Kohn-Sham ansatz, in three parts (here there is no external potential): the kinetic energy of a system of non-interacting electrons, $T^\mathrm{hom}_\mathrm{n.i.}$, the Hartree energy $E^\mathrm{hom}_\mathrm{H}$, and the exchange-correlation energy $E^\mathrm{hom}_\mathrm{xc}$ which is, by definition, all that remains :

$$E^\mathrm{hom}_\mathrm{xc}[\boldsymbol{\rho}] = E^\mathrm{hom}_\mathrm{tot}[\boldsymbol{\rho}] - T^\mathrm{hom}_\mathrm{n.i.}[\boldsymbol{\rho}] - E^\mathrm{hom}_\mathrm{H}[\rho] \tag{9}$$

Given that $T^\mathrm{hom}_\mathrm{n.i.}[\boldsymbol{\rho}]$ and $E^\mathrm{hom}_\mathrm{H}[\rho]$ are straightforward to calculate, an approximation to $E^\mathrm{hom}_\mathrm{tot}[\boldsymbol{\rho}]$ yields an approximation to $E^\mathrm{hom}_\mathrm{xc}[\boldsymbol{\rho}]$.

Analytic approximations to $E^\mathrm{hom}_\mathrm{xc}[\rho]$ have proven successful. In particular, in the first paper to introduce the LSDA[3] von Barth and Hedin presented an analytic calculation of the exchange-correlation energy and potential, including a suitable parametrization. This result, with a slightly different parametrization, was successfully applied to the calculation of electronic properties of metals (including effects of spin polarization).[4] A more accurate calculation of $E^\mathrm{hom}_\mathrm{tot}[\boldsymbol{\rho}]$, based on a quantum Monte Carlo method, was given by Ceperley and Alder,[5] the exchange-correlation part of which was parametrized by Vosko, Wilk and Nusair.[6] This is the most commonly used parametrization of LSDA, although in practice there is little difference in calculated material properties among the three parametrizations of LSDA.[3,4,6] Larger differences, usually towards increased accuracy, are provided when density gradient correction are included within the generalized gradient approximation (GGA).[7]

4 Magnetic Excitations and the Adiabatic Approximation

Density functional calculations reproduce, in many cases with remarkable accuracy, the ground-state magnetic moments of elemental or alloyed systems. Transition-metal ferromagnets (Fe, Co, Ni) and ferromagnetic metallic alloys (e.g. Heusler alloys, such as NiMnSb or Co_2MnSi), magnetic surfaces and interfaces are among the systems that are rather well described within the LSDA or GGA (with an accuracy of a few percent in the magnetic moment). On the other hand, materials where strong correlations play an important role, such as f-electron systems or antiferromagnetic transition metal oxides are not properly described within the LSDA or GGA, but in many cases corrections can be made by including additional semi-empirical terms in the energy and potential (as in the LSDA+U scheme).[8] As an example of the accuracy of the LSDA in the magnetic properties of transition metal alloys, fig. 1 shows experimental and theoretical results on the magnetic moments of Iron-, Cobalt-, and Nickel-based alloys.[9]

However, density functional theory is, in principle, a ground-state theory—at least in its usual, practical implementation. This means that the various approximations to the exchange-correlation potential, when applied, yield approximate values of ground-state energy, charge-density, magnetization, etc. Nevertheless, physical arguments can be used to derive also properties of excited states from DFT calculations. A basis for this is the *adiabatic approximation* (or *adiabatic hypothesis*), i.e., that the energies of some excitations, governed by characteristic frequencies much smaller than the ones of intra- and inter-site electron hopping, can be approximated by ground-state calculations. The adiabatic hypothesis is most often used in the calculation of phonon spectra, ab-initio molecular dynamics, or magnetic excitations.

In magnetic materials, two types of magnetic excitations can be distinguished: (i) the Stoner-type, or longitudinal, where the absolute value of the atomic moments changes, and (ii) the Heisenberg-type, or transverse, where the relative direction of the moments changes. Longitudinal excitations usually require high energies, of the order of the intra-atomic exchange (order of 1 eV); clearly this energy scale is far beyond the Curie temperature (ferromagnetic fcc Cobalt has the highest known Curie temperature at 1403 K, while 1 eV corresponds to 11605 K). Transverse excitations (magnons), on the other hand, are one or two orders of magnitude weaker, and are responsible for the ferromagnetic-paramagnetic phase transition.

The characteristic time scale of magnons is of the order of 10^{-12} seconds. On the other hand, inter-atomic electron hopping takes place in timescales of the order of 10^{-15} seconds. As a result, during the time that it takes a magnon to traverse a part of the system, it is expected that locally the electron gas has time to adjust and relax to a new ground state, defined by a constrained, position-dependent magnetization direction. This is the adiabatic hypothesis. For practical calculations, this means that the magnon energy can be found by using an additional position-dependent magnetic field to constrain the magnetic configuration to a magnon-like form (a so-called spin spiral), and calculating the resulting total energy. It should be noted here that the magnon energy arises from the change in electron inter-site hopping energy.

Essentially, the adiabatic hypothesis directs us to approximate the excited-state energy of one system (e.g., a ferromagnet) by the ground-state energy of a different system (a ferromagnet under the influence of constraining fields).

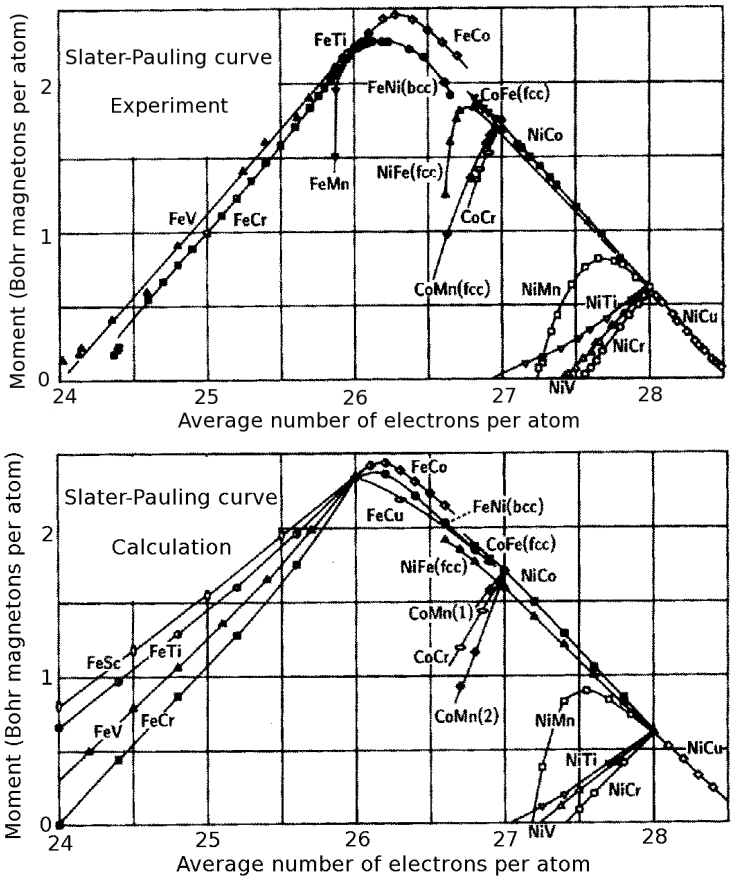

Figure 1. Magnetic moments of Fe, Co and Ni based transition-metal alloys, taken from Dederichs et al.[9] The theoretical results were calculated within the LSDA, using the Korringa-Kohn-Rostoker Green function method and the coherent potential approximation for the description of chemical disorder. The magnetization as a function of average number of electrons per atom follows the *Slater-Pauling rule*.

5 Calculations within the Adiabatic Hypothesis

In this section we discuss how the adiabatic hypothesis can be practically used to extract excited state energies from density functional calculations. The accuracy of the method is such that small energy differences, of the order of meV, can be reliably extracted from total energies of the order of thousands of eV; for instance, for fcc Co the calculated total energy per atom is approximately 38000 eV, while the nearest-neighbour exchange coupling is approximately 14 meV. Such accuracy is crucial for the success of the Multiscale Programme.

5.1 Constrained density functional theory for magnetic systems

Constrained DFT[10] includes an additional term to the energy functional, so that the system is forced to a specific configuration. For the case of interest here, the following functional must be minimized in order to obtain a particular configuration of magnetic moments $\{\vec{M}_n\}$:

$$E_{\mathrm{CDFT}}[\boldsymbol{\rho}; \{\vec{M}_n\}] = E_{\mathrm{DFT}}[\boldsymbol{\rho}] - \sum_n \int_{\text{Cell n}} d^3r\, \vec{H}_n \cdot \left[\vec{m}(\vec{r}) - \vec{M}_n\right]. \tag{10}$$

In this expression, $E_{\mathrm{DFT}}[\boldsymbol{\rho}]$ is the DFT energy functional (1) (e.g., in the LSDA or GGA), while the quantities $\{\vec{H}_n\}$ are Lagrange multipliers, physically interpreted as external magnetic fields acting in the atomic cells $\{n\}$; for convenience in notation we define $\vec{H}_n$ to be constant in the atomic cell n and zero outside. Furthermore, $\vec{m}(\vec{r})$ is the spin density, while $\vec{M}_n$ is the desired magnetic moment. Application of the Raleygh-Ritz variational principle to eq. (10) leads to the Schrödinger-like equation:

$$\left(-\frac{\hbar^2}{2m}\nabla^2 + V_{\text{eff}}(\vec{r}) + \vec{\boldsymbol{\sigma}} \cdot \vec{B}_{\text{eff}}(\vec{r}) + \vec{\boldsymbol{\sigma}} \cdot \sum_n \vec{H}_n - E_i\right) \begin{pmatrix} \psi_{i\uparrow}(\vec{r}) \\ \psi_{i\downarrow}(\vec{r}) \end{pmatrix} = 0. \tag{11}$$

This is just the Kohn-Sham equation (2) with an additional term containing the Lagrange multipliers $\vec{H}_n$ which act as an external Zeeman magnetic field (note that this is not really a magnetic field, in the sense that it is not associated to a vector potential, Landau levels, etc.). In practice, $\vec{H}_n$ is specified and the corresponding value of $\vec{M}_n$ is an output of the self-consistent calculation, calculated from the spin density as

$$\vec{M}_n = \int_{\text{Cell n}} d^3r\, \vec{m}(\vec{r}). \tag{12}$$

If a particular value of $\vec{M}_n$ is to be reached, then $\vec{H}_n$ has to be changed and $\vec{M}_n$ recalculated, until $\vec{M}_n$ reaches the pre-defined value. At the end the energy-functional minimization yields the density $\boldsymbol{\rho}_{\min}$, obeying the condition (12). Since the multipliers $\{\vec{H}_n\}$ enter equation (11) as external parameters, it is evident that the minimizing density $\boldsymbol{\rho}_{\min}$ and the constrained ground-state energy $E_{\mathrm{CDFT}}[\boldsymbol{\rho}_{\min}; \{\vec{M}_n\}]$ are functions of $\{\vec{H}_n\}$. Therefore, to simplify the notation when referring to the constrained ground state, we write $\boldsymbol{\rho}_{\min} = \boldsymbol{\rho}_{\min}[\{\vec{H}_n\}]$, $E_{\mathrm{CDFT}}[\boldsymbol{\rho}_{\min}; \{\vec{M}_n\}] = E_{\mathrm{CDFT}}[\{\vec{H}_n\}]$. Similarly, the multipliers $\{\vec{H}_n\}$ are functions of the constrained ground-state moments, and vice versa: $\vec{H}_n = \vec{H}_n[\{\vec{M}_m\}]$, $\vec{M}_n = \vec{M}_n[\{\vec{H}_m\}]$.

The total energy of the constrained state is given by

$$E_{\mathrm{tot}}^{\mathrm{constr}}(\{\vec{M}_n\}) := E_{\mathrm{CDFT}}[\{\vec{H}_n\}] = E_{\mathrm{DFT}}\left[\boldsymbol{\rho}_{\min}[\{\vec{H}_n\}]\right] \tag{13}$$

(the latter step, where the constrained ground-state density $\boldsymbol{\rho}_{\min}[\{\vec{H}_n\}]$ is taken as argument of the unconstrained density functional E_{DFT}, follows because the last part of eq. (10) vanishes for the self-consistent solution). In order to extract the excited state energy from eq. (13), a subtraction of the unconstrained-state energy from the constrained one is needed:

$$\Delta E[\{\vec{M}_n\}] = E_{\mathrm{CDFT}}[\{\vec{H}_n\}] - E_{\mathrm{CDFT}}[\{\vec{H}_n\} = 0] \tag{14}$$

$$= E_{\mathrm{tot}}^{\mathrm{constr}}[\{\vec{M}_n\}] - E_{\mathrm{tot}}^{0} \tag{15}$$

This can be susceptible to numerical errors, as the total energies are large quantities compared to the change in magnetization energy. There is an alternative to that route.[10,11] By taking advantage of the Helmann-Feynman theorem,

$$\frac{\partial E_{\mathrm{CDFT}}[\boldsymbol{\rho}_{\mathrm{min}}; \{\vec{M}_m\}]}{\partial \vec{M}_n} = \vec{H}_n, \tag{16}$$

which rests on the variational nature of the energy around $\boldsymbol{\rho}_{\mathrm{min}}$, the energy difference can be calculated by an integration along a path from the ground-state moments $\vec{M}_n^{\mathrm{GS}} = \vec{M}_n[\{\vec{H}_m\} = 0]$ to the constrained end-state moments $\vec{M}_n$. Along this path, the Lagrange multipliers $\vec{H}_n[\{\vec{M}_m\}]$ are found by minimization of the constrained energy functional. We have:

$$E_{\mathrm{CDFT}}[\{\vec{H}_n\}] - E_{\mathrm{CDFT}}[\{\vec{H}_n\} = 0] = \sum_n \int_{\vec{M}_n^{\mathrm{GS}}}^{\vec{M}_n} d\vec{M}'_n \cdot \vec{H}_n[\{\vec{M}'_m\}]. \tag{17}$$

It should be noted, however, that this method can be numerically more expensive, as a number of self-consistent calculations are necessary along the path in order to obtain an accurate integration. In practice, the former method of total energy subtraction usually works rather well as long as care is taken for good spin-density convergence in the self-consistent cycle.

5.2 Magnetic force theorem

In principle, to find the excited-state energy $E^{\mathrm{tot}}_{\mathrm{constr}}[\{\vec{M}_n\}]$ one must perform a self-consistent calculation for the particular moments configuration $\{\vec{M}_n\}$. This can be computationally expensive. Fortunately, under certain conditions additional self-consistent calculations can be avoided by virtue of the *force theorem*.[12,13] This states that, under sufficiently small perturbations of the (spin) density, the total energy difference can be approximated by the difference of the occupied single-particle state energies, given by (7). As a consequence, for the total energy difference between the magnetic ground state and the magnetic state characterized by rotated moments $\{\vec{M}_n\}$, one has merely to perform a position-dependent rotation of the ground-state spin density $\vec{m}(\vec{r})$ to a new spin density $\vec{m}'(\vec{r})$ at each atom so that eq. (12) is satisfied, calculate the single-particle energies sum at this non-self-consistent spin density, and subtract the single-particle energies sum of the ground state:

$$\Delta E[\{\vec{M}_n\}] \simeq E_{\mathrm{sp}}[\rho, \vec{m}'] - E_{\mathrm{sp}}[\rho, \vec{m}]. \tag{18}$$

The calculation of $E_{\mathrm{sp}} = \sum_{E_i \leq E_{\mathrm{F}}} E_i$ requires the solution of eq. (11) (or eq. (2)), where the potentials V_{eff} and $\vec{B}_{\mathrm{eff}}$ enter explicitly instead of the densities ρ and $\vec{m}$. Therefore, in practice, the magnetic exchange-correlation potentials $\vec{B}_{\mathrm{eff}}$ are rotated for the energy estimation in eq. (18), instead of the spin density $\vec{m}$.

5.3 Reciprocal space analysis: generalized Bloch theorem

The elementary, transverse magnetic excitations in ferromagnetic crystals have, in a semi-classical picture, the form of spin spirals of wave-vector $\vec{q}$. If the ground-state magnetization M_0 is oriented along the z-axis, then in the presence of a spin spiral the spin density

and the exchange-correlation potential at the atomic cell at lattice point $\vec{R}_n$ are given in terms of a position-dependent angle $\phi_n = \vec{q}\cdot\vec{R}_n$ and an azimuthal angle θ:

$$\vec{m}(\vec{r}+\vec{R}_n) = m_0(\vec{r})\left(\sin\theta\,\cos(\vec{q}\cdot\vec{R}_n)\,\hat{x} + \sin\theta\,\cos(\vec{q}\cdot\vec{R}_n)\,\hat{y} + \cos\theta\,\hat{z}\right) \quad (19)$$

$$\vec{B}(\vec{r}+\vec{R}_n) = B_0(\vec{r})\left(\sin\theta\,\cos(\vec{q}\cdot\vec{R}_n)\,\hat{x} + \sin\theta\,\cos(\vec{q}\cdot\vec{R}_n)\,\hat{y} + \cos\theta\,\hat{z}\right) \quad (20)$$

This implies that the potential has a periodicity of the order of $1/q$, thus, for small q, the unit cell contains too many atoms to handle computationally. However, there is a *generalized Bloch theorem*,[14] by virtue of which the calculation can be confined to the primitive unit cell. The generalized Bloch theorem is valid under the assumption that the hamiltonian $\mathcal{H}$ (or equivalently the potential) obeys the transformation rule

$$\mathcal{H}(\vec{r}+\vec{R}_n) = \mathbf{U}(\vec{q}\cdot\vec{R}_n)\mathcal{H}(\vec{r})\mathbf{U}^{\dagger}(\vec{q}\cdot\vec{R}_n). \quad (21)$$

with the spin transformation matrix $\mathbf{U}$ defined by

$$\mathbf{U}(\vec{q}\cdot\vec{R}^n) = \begin{pmatrix} e^{-i\vec{q}\cdot\vec{R}_n/2} & 0 \\ 0 & e^{i\vec{q}\cdot\vec{R}_n/2} \end{pmatrix}. \quad (22)$$

This is true if the exchange-correlation potential has the form (20) and if the spin orbit coupling can be neglected. This transformation rule in spin space has as a consequence that the hamiltonian remains invariant under a *generalized translation* $\mathcal{T}_n = T_n\,\mathbf{U}(\vec{q}\cdot\vec{R}^n)$ which combines a translation in real space by the lattice vector $\vec{R}_n$, T_n, with a rotation in spin space, $\mathbf{U}(\vec{q}\cdot\vec{R}_n)$:

$$\mathcal{T}_n\,\mathcal{H}\,\mathcal{T}_n^{-1} = \mathcal{H}. \quad (23)$$

As a result of this invariance, using manipulations analogous to the ones that lead to the well-known Bloch theorem it can be shown that the spinor eigenfunctions are of the form

$$\psi_{\vec{k}}(\vec{r}) = e^{i\vec{k}\cdot\vec{r}}\begin{pmatrix} e^{-i\vec{q}\cdot\vec{r}}\,\alpha_{\vec{k}}(\vec{r}) \\ e^{+i\vec{q}\cdot\vec{r}}\,\beta_{\vec{k}}(\vec{r}) \end{pmatrix} \quad (24)$$

where $\alpha_{\vec{k}}(\vec{r})$ and $\beta_{\vec{k}}(\vec{r})$ are lattice-periodic functions, $\alpha_{\vec{k}}(\vec{r}+\vec{R}_n) = \alpha_{\vec{k}}(\vec{r})$ and $\beta_{\vec{k}}(\vec{r}+\vec{R}_n) = \beta_{\vec{k}}(\vec{r})$. In this way, given a particular spin-spiral vector $\vec{q}$, the calculation is confined in the primitive cell in real space (and in the first Brillouin zone in k-space) and is thus made computationally tractable.

In case that the atomic magnetic moments do not change appreciably under rotation, the energy differences $\Delta E(\vec{q};\theta)$ can be Fourier-transformed[15] in order to find the real-space excitation energies $\Delta E[\{\vec{M}_n\}]$. This is usually true when θ is small. Under this condition, the force theorem is also applicable, so that non-self-consistent calculations are sufficient to find the dispersion relation $\Delta E(\vec{q};\theta)$ for $\vec{q}$ in the Brillouin zone.

5.4 Real space analysis: Green functions and the method of infinitesimal rotations

For perturbations that are confined in space, the Green function method is most appropriate for the calculation of total energies. The reason is that it makes use of the Dyson equation for the derivation of the Green function of the perturbed system from the Green function of the unperturbed system, with the correct open boundary conditions taken into account

automatically. As opposed to this, in wave function methods for localized perturbations a solution of the Scrödinger (or Kohn-Sham) equation requires explicit knowledge of the boundary condition and a complicated coupling procedure in order to achieve continuity of the wavefunction and its first derivative at the boundary.

The Green function $\boldsymbol{G}(\vec{r},\vec{r}\,';E)$ corresponding to the Kohn-Sham hamiltonian of eq. (2) is a 2×2 matrix in spin space that obeys the equation

$$\left(-\tfrac{\hbar^2}{2m}\nabla^2+V_{\rm eff}(\vec{r})+\vec{\boldsymbol{\sigma}}\cdot\vec{B}_{\rm eff}(\vec{r})-E\right)\begin{pmatrix}G_{\uparrow\uparrow}(\vec{r},\vec{r}\,';E)\;G_{\uparrow\downarrow}(\vec{r},\vec{r}\,';E)\\ G_{\downarrow\uparrow}(\vec{r},\vec{r}\,';E)\;G_{\downarrow\downarrow}(\vec{r},\vec{r}\,';E)\end{pmatrix} = -\begin{pmatrix}1\;0\\0\;1\end{pmatrix}\delta(\vec{r}-\vec{r}\,'). \tag{25}$$

The particle density and spin density can be readily calculated from $\boldsymbol{G}$ as

$$\rho(\vec{r}) = -\frac{1}{\pi}{\rm Im}\int^{E_{\rm F}} dE\,{\rm Tr}_s\,\boldsymbol{G}(\vec{r},\vec{r}\,';E) \tag{26}$$

$$\vec{m}(\vec{r}) = -\frac{1}{\pi}{\rm Im}\int^{E_{\rm F}} dE\,{\rm Tr}_s\,[\vec{\boldsymbol{\sigma}}\,\boldsymbol{G}(\vec{r},\vec{r}\,';E)] \tag{27}$$

where ${\rm Tr}_s$ indicates a trace over spins. More generally, the Green function corresponding to a hamiltonian $\mathcal{H}$ obeys the equation $(E-\mathcal{H})\,\mathcal{G}(E)=1$. In case of a perturbation $\Delta\mathcal{V}$ to a hamiltonian $\mathcal{H}_0$, the Green function $\mathcal{G}(E)=(E-\mathcal{H})^{-1}$ to the new hamiltonian, $\mathcal{H}=\mathcal{H}_0+\Delta\mathcal{V}$, is related to the initial Green function, $\mathcal{G}_0(E)=(E-\mathcal{H}_0)^{-1}$, via the Dyson equation $\mathcal{G}(E)=\mathcal{G}_0(E)\,[1-\Delta\mathcal{V}\,\mathcal{G}_0(E)]^{-1}$. In practice, the latter equation is very convenient to use because it requires a minimal basis set. With some reformulation the Dyson equation forms the basis of the Korringa-Kohn-Rostoker (KKR) Green function method for the calculation of the electronic structure of solids[16] and impurities in solids.[17] Within the KKR method, the Green function is expanded in terms of regular ($R^n_{s;L}(\vec{r};E)$) and irregular ($H^n_{s;L}(\vec{r};E)$) scattering solutions of the Schrödinger equation for the atomic potentials embedded in free space. The index n denotes the atom, $L=(l,m)$ stands for a combined index for the angular momentum quantum numbers of an incident spherical wave, and s is the spin ($\uparrow$ or $\downarrow$). For a ferromagnetic system, where only spin-diagonal elements of the Green function exist, $G_{ss'}=G_s\delta_{ss'}$ in (25), the expansion reads:

$$\begin{aligned}G_s(\vec{r}+\vec{R}_n,\vec{r}\,'+\vec{R}_{n'};E) = -i\sqrt{\frac{2mE}{\hbar^2}}\sum_L R^n_{s;L}(\vec{r};E)H^n_{s;L}(\vec{r}\,';E)\,\delta_{nn'}\\ +\sum_{LL'}R^n_{s;L}(\vec{r};E)\,G^{nn'}_{s;LL'}(E)\,R^{n'}_{s;L'}(\vec{r}\,';E)\end{aligned} \tag{28}$$

for $|\vec{r}|<|\vec{r}\,'|$ (for $|\vec{r}|>|\vec{r}\,'|$, $\vec{r}$ and $\vec{r}\,'$ should be interchanged in the first term of the RHS). The coefficients $G^{nn'}_{s;LL'}(E)$ are called structural Green functions and are related to the structural Green functions of a reference system (e.g., free space) via an algebraic Dyson equation[16,17] which involves the spin-dependent scattering matrices $t^n_{s;LL'}(E)$. In case of a non-collinear magnetic perturbation in a ferromagnetic system, the method can be generalized in a straightforward way[13,18] yielding the total energy of the state, $E[\{\vec{M}_n\}]$. However, in the limit of infinitesimal rotations of the moments $\{\vec{M}_n\}$, perturbation theory can be employed in order to find the change in the density of states, and by application

of the force theorem, the change in total energy. Of particular interest for our discussion below is the result for the total energy change in second order when two moments $\vec{M}_n$ and $\vec{M}_{n'}$ are infinitesimally rotated:[19]

$$\frac{\delta^2 E}{\delta\vec{M}_n \delta\vec{M}_{n'}} = -\frac{1}{8\pi\,|\vec{M}_n|\,|\vec{M}_{n'}|}\mathrm{Im}\int^{E_\mathrm{F}} dE\,\mathrm{Tr}_L\left[\boldsymbol{G}_\uparrow^{nn'}\,(\boldsymbol{t}_\uparrow^{n'}-\boldsymbol{t}_\downarrow^{n'})\,\boldsymbol{G}_\uparrow^{n'n}\,(\boldsymbol{t}_\uparrow^{n}-\boldsymbol{t}_\downarrow^{n})\right] \tag{29}$$

In this formula, $\boldsymbol{G}_s^{nn'}(E)$ is the structural Green function of spin s in form of a matrix in L, L', while $\boldsymbol{t}_s^n(E)$ are again the scattering matrices. Tr_L denotes a trace in angular momentum quantum numbers. The derivatives on the LHS are implied to be taken only with respect to the angles of $\vec{M}_n, \vec{M}_{n'}$, not the magnitude.

6 Correspondence to the Heisenberg Model

The next step of the Multiscale Programme is to establish a correspondence between the density functional results and the parameters of a phenomenological model hamiltonian for magnetism. Usually, the classical Heisenberg model is used in order to derive the magnetism-related statistics up to (and even beyond) the Curie temperature, and we will focus on this. However, other models can be used for different purposes, such as the continuum model for micromagnetic or magnetization dynamics calculations. Also, even on the atomic scale, it is sometimes necessary to extend the Heisenberg model to non-rigid spins.

The classical Heisenberg hamiltonian for a system of magnetic moments $\{\vec{M}_n\}$ is

$$\mathcal{H} = -\frac{1}{2}\sum_{nn'} J_{nn'}\vec{M}_n\vec{M}_{n'}. \tag{30}$$

The quantities $J_{nn'}$ are called pair exchange constants, and they are assumed to be symmetric ($J_{nn'} = J_{n'n}$), while, by convention, $J_{nn} = 0$. The prefactor $1/2$ takes care of double-counting. The exchange constants fall off sufficiently fast with distance, so that only a finite amount of neighbours n' has to be considered in the sum for each n. Physically, it is well known that the exchange interaction results from the change of the electronic energy under rotation of the moments, not from the dipole-dipole interaction of the moments.

A correspondence to density functional calculations can be made due to the observation that

$$J_{nn'} = -\frac{\partial^2\mathcal{H}}{\partial\vec{M}_n\partial\vec{M}_{n'}} \tag{31}$$

assuming that, to a good approximation, the constrained DFT energy can be expanded to lowest order in the moments' angles as $E_\mathrm{tot}^\mathrm{constr}[\{\vec{M}_n\}] - E_\mathrm{tot}^0 = -\frac{1}{2}\sum_{nn'} J_{nn'}\vec{M}_n\vec{M}_{n'} +$ const. By computing $E[\{\vec{M}_n\}]$ within constrained DFT, the RHS can be evaluated, and $J_{nn'}$ can be found. Thus, the step from DFT to the Heisenberg model relies on accepting the equivalence of the DFT and Heisenberg-model excitation energies. As an example we see in fig. 2 the exchange constants of fcc Cobalt as a function of distance.

Additional terms to the Heisenberg hamiltonian (30) can also be evaluated in a similar way. For instance, the magnetocrystalline anisotropy energy is phenomenologically

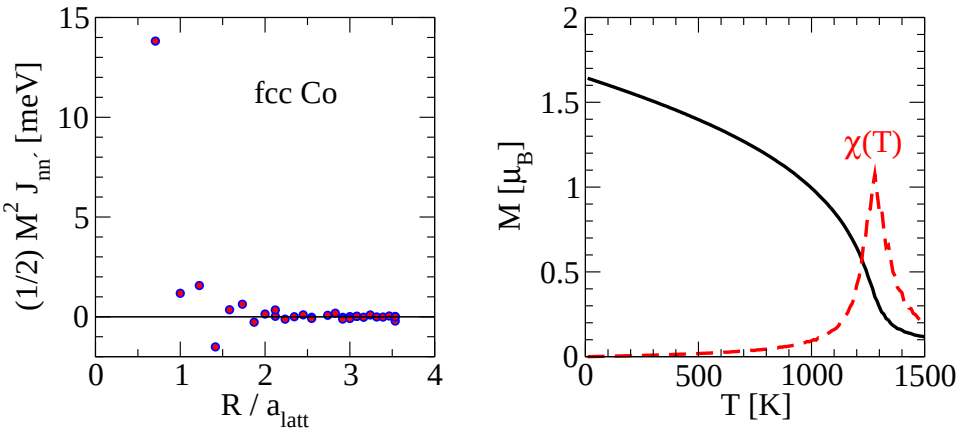

Figure 2. Left: Exchange constants as a function of inter-atomic distance in fcc Co calculated by the method of infinitesimal rotations. Right: Magnetization (in μ_B per atom) and susceptibility χ as functions of temperature, calculated by a Monte Carlo method using the exchange constants of the left panel. The peak of susceptibility signals the Curie temperature. In the simulation a supercell of 1728 atoms was used. The experimentally found Curie temperature is 1403 K.

described by adding the term $-K\sum_n(\vec{M}_n\cdot\hat{\zeta})^2 = -KM\sum_n\cos^2\gamma_n$, where $\hat{\zeta}$ is a unit vector, usually along a high-symmetry crystal axis, and γ_n is the angle of the magnetic moment to this axis. The magnetocrystalline anisotropy, which stems from the spin-orbit coupling, induces the preference of a particular direction for the magnetic moments ($\pm\hat{\zeta}$), if $K > 0$, or in the plane perpendicular to this direction, if $K < 0$. By observing that $K = \frac{1}{2M}\partial^2\mathcal{H}/\partial\gamma^2|_{\gamma=0}$, the constant K can be harvested by fitting DFT total-energy results to the second derivative $\partial^2 E_{\mathrm{CDFT}}[\{\vec{M}_n\}]/\partial\gamma^2|_{\gamma=0}$. Furthermore, in all cases the validity of the phenomenological model can also be subjected to verification by DFT calculations.

Having established the correspondence to the Heisenberg model, there are two practical, widely used ways to calculate the exchange constants $J_{nn'}$. The first, used within Green function methods (KKR or linearized muffin-tin orbital (LMTO) Green function), is a direct combination of eqs. (29) and (31). The second, used within hamiltonian methods, is a Fourier transform of the spin-spiral energy $\Delta E(\vec{q};\theta)$.[15] It should be noted, however, that the assumption of rigid magnetic moment magnitudes, inherent in the Heisenberg model, is only an approximation. When the moment angles between nearest-neighbour atoms become large, the moments can change and the Heisenberg hamiltonian is not any more valid. The extent of this strongly depends on the material, as has been found by DFT calculations; therefore, the Heisenberg hamiltonian should only be considered as the lowest order expansion in the moments.

According to these considerations, the method of infinitesimal rotations should be ideal for calculating the $J_{nn'}$, while the Fourier transform of $\Delta E(\vec{q};\theta)$ is accurate only when θ is chosen small enough. However, this is not the whole story. At high temperatures, close to the Curie temperature, neighbouring moments can have larger respective angles, perhaps of the order of 30 degrees or more. Therefore some sort of "intelligent averaging" over

angles is called for, in order to increase the accuracy of results. The method of infinitesimal rotations can be systematically amended in this direction, as was proposed by Bruno,[20] while for the Fourier-transform method larger angles θ (perhaps of the order of 30 degrees) should be considered. We will return to this discussion in Section 8. We should also mention that the formalism, as it is presented in the present manuscript, neglects the orbital moments and their interaction. Such effects can become important especially for rare earths and actinides, which are, however, not well-described by local density functional theory due to the strong electron correlations in these systems.

7 Solution of the Heisenberg Model

Having established the correspondence between DFT results and the Heisenberg hamiltonian, and having identified the model parameters, a statistical-mechanical method is used in order to solve the Heisenberg model, if one is interested in thermodynamic properties, or a dynamical method is used if one is interested in time-dependent properties. In the former case, the Monte Carlo method, mean-field theory, and the random phase approximation (RPA) are most commonly used. For time-dependent properties we give a brief introduction to Landau-Lifshitz spin dynamics.

7.1 Thermodynamic properties and the Curie temperature

The Monte Carlo method is a stochastic approach to the solution of the Heisenberg model (and of course to many other problems in physics). It is based on a random walk in the configuration space of values of $\{\vec{M}_n\}$, but with an intelligently chosen probability for transition from each state to the next. The random walk must fulfill two requirements: (i) it must be ergodic, i.e., each point of the configuration space must be in principle accessible during the walk, and (ii) the transition probability between states A and B, $t_{A\to B}$, must obey the detailed balance condition, i.e., $P(A)\,t_{A\to B} = P(B)\,t_{B\to A}$, where $P(X) = \exp(-E(X)/k_{\mathrm{B}}T)$ is the Boltzmann probability for appearance of state X at temperature T, with $E(X)$ the energy of the state and k_{B} the Boltzmann constant. As long as these requirements are fulfilled, $t_{A\to B}$ is to be chosen in a way that optimizes the efficiency of the method. The most simple and widely-used way is the Metropolis algorithm,[21] in which $t_{A\to B} = P(B)/P(A) = \exp[(E(A) - E(B))/k_{\mathrm{B}}T]$ is taken for $E(A) < E(B)$ and $t_{A\to B} = 1$ otherwise. For further reading on the Monte Carlo method we refer the reader to the book by Landau and Binder.[22]

Within the Monte Carlo method, a simulation supercell is considered, which contains many atomic sites (e.g., $10 \times 10 \times 10$ for simulating a three-dimensional cubic ferromagnetic lattice). At each site, a magnetic moment $\vec{M}_n$ is placed, subject to interactions $J_{nn'}$ with the neighbours. Usually, periodic boundary conditions are taken in order to avoid spurious surface effects. During a Monte Carlo random walk, thermodynamic quantities (magnetization, susceptibility, etc.) are sampled and averaged over the number of steps. In this way it is possible, for instance, to locate the Curie temperature T_{C} of a ferromagnetic-paramagnetic phase transition by the drop of magnetization or by the susceptibility peak. Since the simulation supercell is finite, the magnetization does not fully disappear, and the susceptibility peak overestimates somewhat T_{C}. However, there are ways of correcting for this deficiency, by increasing the supercell size and using scaling arguments.[22] As an

Material	T_C(K) (exp)	T_C(K) (RPA)	T_C(K) (mean-field)	Ref.
Fe bcc	1044	950	1414	(a)
Co fcc	1403	1311	1645	(a)
Ni fcc	624	350	397	(a)
NiMnSb	730	900	1112	(b)
CoMnSb	490	671	815	(b)
Co_2CrAl	334	270	280	(b)
Co_2MnSi	985	740	857	(b)

Table 1. Experimental and calculated Curie temperatures (in Kelvin, within the RPA) of various ferromagnetic materials. Calculated values taken from: (a): Pajda et al,[25] (b): Sasioglu et al.[26]

example we show in fig. 2 the temperature-dependent magnetization and susceptibility of fcc Co calculated within the Monte Carlo method.

Mean-field theory is a physically transparent and computationally trivial way of estimating thermodynamic properties, however it lacks accuracy because it neglects fluctuations. As regards the Curie temperature, it is systematically overestimated by mean-field theory (assuming applicability of the Heisenberg model). Given the exchange interactions $J_{nn'}$ the mean-field result for T_C in a monoatomic crystal has the simple form

$$k_B\, T_C = \frac{1}{3} M^2 \sum_{n'} J_{nn'}. \tag{32}$$

Another widely used method for estimating the Curie temperature is the random phase approximation. It yields results much improved with respect to mean-field theory with only little increase of the computational burden. It is based on the Green function method for the quantum Heisenberg model, where a decoupling is introduced in the Green function equation of motion, as proposed by Tyablikov for $s = \frac{1}{2}$ systems.[23] Further refinements[24,25] of the RPA for higher-spin systems allow the transition to the classical limit by taking $s \to \infty$. The Curie temperature in a monoatomic lattice is then given by

$$\frac{1}{k_B\, T_C} = \frac{3}{2} \frac{1}{N} \sum_{\vec{q}} \frac{1}{E(\vec{q})} \tag{33}$$

where $E(\vec{q})$ is the magnon (or spin-spiral) energy, calculated by a Fourier transform of $J_{nn'}$ or directly by constrained DFT, and N the number of atoms in the system. For multisublattice systems, a modified version of RPA can be used.[26]

7.2 Time-dependent magnetic properties and Landau-Lifshitz spin dynamics

In case that one is interested in the time dependence of the magnetic moments under the influence, e.g., of an external field pulse, the method of magnetization dynamics can be used. The classical equations of motion associated with this method are the Landau-Lifshitz equations for the moments $\{\vec{M}_n\}$,

$$\frac{d\vec{M}_n}{dt} = \vec{H}_n^{\text{eff}} \times \vec{M}_n, \tag{34}$$

$$\vec{H}_n^{\text{eff}} = \sum_{n'} J_{nn'} \vec{M}_{n'} + \vec{H}^{\text{ext}}. \tag{35}$$

These are first-order equations in time which describe the precession of the magnetic moment due to external fields (different than an electric dipole, which will rotate towards the direction of an electric field, the magnetic dipole is essentially an angular momentum and therefore will precess around a magnetic field). The effective field defined in eq. (35) comprises the exchange interaction with the neighbours and an externally applied magnetic field. However, other terms can be included in $\vec{H}_n^{\rm eff}$, such as the magnetocrystalline anisotropy or the magnetic field created by the very moments of the material itself—the latter becomes most important in large ferromagnetic systems, and we discuss in the next subsection.

As is obvious by taking the dot product of eq. (34) with $\vec{M}_n$, $\vec{M}_n \cdot d\vec{M}_n/dt = 0$, i.e., the Landau-Lifshitz equations conserve the magnitude of the moments. They also conserve the total energy. However, dissipation effects that lead to damping of the precession can be taken into account by an additional phenomenological term of the form $\lambda(\vec{H}_n^{\rm eff} \times \vec{M}_n) \times \vec{M}_n$, where a parameter λ describes the damping strength. Temperature effects can also be simulated by additional phenomenological terms of stochastic forces, through an approach similar to Langevin molecular dynamics.[27]

We should note here the existence of a formalism for fully ab-initio spin dynamics, i.e., without the assumption of a Heisenberg model.[28] (From this formalism the Landau-Lifshitz equations follow as a limiting case.) However, this approach is computationally heavy, as it requires self-consistent density functional calculations at each time step of the system evolution.

7.3 Dipolar field calculation and related multiscale modelling

We now discuss the effect of the dipole-dipole interaction on the magnetic configuration. By this we mean the interaction of each magnetic dipole (here, atomic magnetic moment) with the magnetic field created by all other dipoles in the system. It is well-known that the this type of interaction between two moments $\vec{M}_n$ and $\vec{M}_{n'}$, connected by a vector $\vec{R}_{nn'} = \vec{R}_n - \vec{R}_{n'}$, has the form

$$E_{\rm dip}(\vec{R}) = \frac{3\,(\vec{M}_n \cdot \vec{R}_{nn'})(\vec{M}_{n'} \cdot \vec{R}_{nn'}) - (\vec{M}_n \cdot \vec{M}_{n'})\,R_{nn'}^2}{R_{nn'}^5} \tag{36}$$

Equivalently, each moment feels a magnetic field, the *dipolar field* $\vec{H}_n^{\rm dip}$, to be included in $\vec{H}_n^{\rm eff}$ in the Landau-Lifshitz equation, of the form

$$\vec{H}_n^{\rm dip} = \sum_{n' \neq n} \frac{3\,\vec{R}_{nn'}(\vec{M}_{n'} \cdot \vec{R}_{nn'}) - \vec{M}_{n'}\,R_{nn'}^2}{R_{nn'}^5} \tag{37}$$

Compared to the nearest-neighbour exchange interactions $J_{nn'}$, the interaction between two dipoles is weak, but the complication is that the summation (37) cannot be restricted to a few neighbours only, as it falls off relatively slowly with distance ($\sim 1/R_{nn'}^3$). Especially in three-dimensional systems the sum is guaranteed to converge only by finite-size effects of the sample, i.e., it becomes a meso- or macroscopic property and the sample boundaries become important.[a] $\vec{H}_n^{\rm dip}$ is evidently time-consuming to calculate; particularly a brute-force calculation would be impossible for large systems. There are, however,

[a] In large ferromagnetic systems the dipolar field cannot be neglected, as it is responsible for the emergence of magnetic domains.

special techniques that allow for a fast, approximate calculation of $\vec{H}_n^{\rm dip}$. This is even more crucial for spin dynamics, as $\vec{H}_n^{\rm dip}$ depends on the moments configuration and has to be calculated anew at each time step.

One such technique is the *fast multipole method*, originally introduced to treat the problem of Coulombic interactions.[29] The central idea is to divide space in regions of different sizes, and treat the collective field from each region by a multipole expansion up to a certain order. The higher the order, the more accurate and expensive the calculation. Given a certain expansion order, regions that are far away from the point of field-evaluation can be large, while regions that are close have to be smaller to maintain accuracy (the criterion of region size is the opening angle D/R, with D the diameter of the region and R its distance from the point of field-evaluation). An essential ingredient of the fast multipole method is the efficient derivation of multipoles of a large region from the multipoles of its subregions. This derivation requires the calculation of multipole expansion and translation coefficients, which, however, depend only on the geometry and for magnetic systems have to be evaluated only once (as the magnetic moments are not moving).

A fast evaluation of the dipolar field allows for multiscale simulations in magnetostatics[30] or magnetization dynamics, also in a sense that we have not discussed up to this point. In such simulations, the transition from the large (mesoscopic or even macroscopic) scale to the atomic scale is done in a seamless way. The idea is to treat the magnetization as a continuous field by a coarse grained approach in regions where it is relatively smooth, whereas to gradually refine the mesh, even up to the atomic limit, in regions where the spatial fluctuations become more violent (e.g. magnetic vortex cores, Bloch points, monoatomic surface step edges, ferromagnet-antiferromagnet interfaces, etc.). In the continuum limit, however, the Landau-Lifshitz equations (34) must be rewritten in terms of a continuous magnetization $\vec{M}(\vec{r})$ and the *spin stiffness* A:

$$\frac{d\vec{M}(\vec{r})}{dt} = \vec{H}^{\rm eff}(\vec{r}) \times \vec{M}(\vec{r}) \tag{38}$$

$$\vec{H}^{\rm eff}(\vec{r}) = \frac{2}{M_s^2} A \nabla^2 \vec{M}(\vec{r}). \tag{39}$$

$M_s = |\vec{M}(\vec{r})|$ is the absolute value of the continuum magnetization (also called saturation magnetization in ferromagnetic samples). The term $A\nabla^2\vec{M}(\vec{r})$ results from taking $\sum_{n'} J_{nn'}\vec{M}_{n'}$ to the continuum limit; the spin stiffness is given (in an example of a monoatomic crystal with atomic moment M and primitive cell volume V_c) in terms of the exchange constants as $A = (1/4V_c)M^2 \sum_n J_{0n} R_n^2$, with R_n the distance of atom n from the origin.

8 Back-Coupling to the Electronic Structure

So far we have discussed how the transition from the DFT to the Heisenberg model is achieved by fitting the Heisenberg model parameters to DFT total energies at and close to the ground state. However, at higher temperature (close to the Curie temperature, that can be of the order of 1000 K) the local electronic structure can change. Several mechanisms can contribute to this: lattice vibrations, single-electron excitations, collective electronic

excitations such as magnons, structural phase transitions (such as the hcp to fcc transition of Cobalt above 700 K) etc. As a consequence, the pair exchange parameters $J_{nn'}$ calculated from the low-temperature electronic structure could be significantly altered.

Perhaps the most serious effect can be caused by the non-collinear magnetic configurations at high temperature, in which the angle between first-neighbouring moments can be of the order of 30°. At such high angles, and depending on the system, the parametrization of the total energy with respect to the Heisenberg model can be insufficient—recall that, in principle, the Heisenberg hamiltonian is justified as the lowest-order term in an expansion with respect to the angle. An often encountered consequence of an altered local electronic structure is a change of the atomic moments. Furthermore, as this angle is not static, but fluctuating in time, it is no use to simply perform static non-collinear calculations at this angle and derive the $J_{nn'}$ by small deviations. We are thus faced with the problem of a back-coupling of the high-temperature state to the electronic structure; i.e., of approximating the local electronic properties in the presence of thermal fluctuations.

Two solutions are frequently used to this problem. The first is to go beyond the Heisenberg model and perform a more thorough parametrization of the energy as a function of the moments, including also possible changes in the magnitude of the moments. This method has been applied, e.g., by Uhl and Kübler.[31] The disadvantage is that it can be computationally expensive, both due to the number of self-consistent constrained-DFT calculations required for a parametrization of the multi-dimensional space $\{\vec{M}_n\}$, and because of the more involved Monte Carlo calculations where the change of the moments magnitude has to be accounted for. There are, however, reasonable approximations that can reduce the necessary number of parameters, while the Curie temperature can be found within a modified mean-field theory.[31]

The second solution is to assume that the Heisenberg model is still adequate to describe the phase transition, but with "renormalized" parameters, chosen such that the change of the local electronic structure is taken into account by an averaging over angles. This solution is intuitive but certainly not rigorous. It is, however, simple to include within Green function electronic structure methods, by assuming an analogy of the high-temperature state with a spin-glass state and employing the coherent potential approximation (CPA). Spin-glass systems are characterized by *disordered local moment* (DLM) states, consisting of two different magnetic "species" that correspond, say, to the magnetic moment pointing "up" (A) or "down" (B). These are encountered in a random manner with a probability $1-x$ and x, respectively: the DLM state is of the form $A_{1-x}B_x$. For $x=0$ we recover the ferromagnetic state, while for $x=0.5$ we have complete magnetic disorder. (Note that a DLM state is different than the antiferromagnetic state, in which the species A and B are well-ordered in two sublattices.) Under the assumption of an analogy of high-temperature states in ferromagnets to DLM systems, the ferromagnet at the Curie temperature is approximated by the alloy $A_{0.5}B_{0.5}$.

The CPA is a method for the description of chemical disorder in alloys, and can be applied here to the magnetic type of alloy $A_{0.5}B_{0.5}$. Within the CPA, the Green function $\bar{\boldsymbol{G}}$ and scattering matrix $\bar{\boldsymbol{t}}$ of an effective average medium are sought, such that the additional scattering of atoms A and B in this medium vanishes on the average. We skip the derivation, which can be found in many textbooks,[32,33] and give only the final CPA condition

that has to be fulfilled:

$$\bar{\boldsymbol{t}}^{-1} = (1-x)\,\boldsymbol{t}_A^{-1} + x\,\boldsymbol{t}_B^{-1} + (\bar{\boldsymbol{t}}^{-1} - \boldsymbol{t}_A^{-1})(\bar{\boldsymbol{t}}^{-1} - \bar{\boldsymbol{G}})^{-1}(\bar{\boldsymbol{t}}^{-1} - \boldsymbol{t}_B^{-1}), \tag{40}$$

$$\bar{\boldsymbol{G}} = \boldsymbol{g}\,\left(1 - \bar{\boldsymbol{t}}\boldsymbol{g}\right)^{-1} \tag{41}$$

with $\boldsymbol{g}$ the free-space structural Green function in the KKR formalism.[16] Expression (41) is the Dyson equation for the Green function of the average medium, which depends on the average-medium scattering matrix $\bar{\boldsymbol{t}}$. The latter is determined by Eq. (40), which contains $\bar{\boldsymbol{t}}$ also on the right-hand side (explicitly and also through $\bar{\boldsymbol{G}}$), and is solved self-consistently by iteration. At the end, the Green functions of species A and B are projected out from the average medium Green function again via the Dyson equation

$$\boldsymbol{G}_{A,B} = \bar{\boldsymbol{G}}\,\left(1 - (\boldsymbol{t}_{A,B} - \bar{\boldsymbol{t}})\,\bar{\boldsymbol{G}}\right)^{-1} \tag{42}$$

and used for the calculation of the electronic structure of the two atomic species.

Given the CPA Green function for the $A_{0.5}B_{0.5}$ DLM state, the method of infinitesimal rotations can be employed to obtain the pair exchange constants. Assuming that the DLM state represents the magnetic structure at the Curie temperature, the exchange constants obtained by this method should be more appropriate to use in the Heisenberg hamiltonian close to T_{C} than the ones obtained from the ground state. However, this is not guaranteed, especially in view of the fact that the CPA neglects the short-range magnetic order that is present even at T_{C}.

9 Concluding Remarks

The Multiscale Programme discussed here is widely used today, however, the matter is surely not closed. Mainly two types of difficulties are present and are the subject of current research. First, density functional theory within the local spin density or generalized gradient approximation is not able to describe the ground state properties of every material. When electron correlations (on-site electron-electron repulsion and temporal electron density fluctuations) become particularly strong, these approximations fail. Characteristic of such problems are f-electron systems, transition metal oxides or molecular magnets. Improved concepts exist and are applied, such as the LSDA+U or dynamical mean-field theory, however, at the moment these methods rely on parameters that cannot always be found without a fit to experiment.

Second, the excited state properties are also not always accessible to density functional theory. The adiabatic hypothesis, together with constrained DFT, work up to a point, but effects as the magnon lifetime or frequency-dependent interactions are neglected. Current work in this direction is done within approximations as the GW or time-dependent DFT, with promising results. These methods are, however, still computationally very expensive, and the extent of improvement that they can offer to the calculation of thermodynamical properties remains unexplored.

Acknowledgments

I am grateful to D. Bauer, S. Blügel, P.H. Dederichs, R. Hertel, M. Ležaić, S. Lounis, and L.M. Sandratskii for illuminating discussions on the subjects presented in this work.

References

1. P. Hohenberg and W. Kohn Phys. Rev. **136**, B864 (1964).
2. W. Kohn and L. J. Sham Phys. Rev. **140**, A1133 (1965).
3. U. von Barth and L. Hedin, J. Phys. C: Solid State Phys. **5**, 1629 (1972).
4. V.L. Moruzzi, J.F. Janak, and A.R. Williams, *Calculated electronic properties of metals* (Pergamon, New York 1978).
5. D.M. Ceperley and B.J. Alder, Phys. Rev. Lett. **45**, 566 (1980).
6. S.H. Vosko, L. Wilk, and M. Nusair, Can. J. Phys. **58**, 1200 (1980).
7. See, for example, J.P. Perdew, K. Burke, and Y. Wang, Phys. Rev. B **54**, 16533 (1996); J.P. Perdew, K. Burke, and M. Ernzerhof, Phys. Rev. Lett. **77**, 3865 (1996).
8. V.I. Anisimov, F. Aryasetiawan, and A.I. Lichtenstein J. Phys.: Condens. Matter **9**, 767 (1997).
9. P.H. Dederichs, R. Zeller, H. Akai, and H. Ebert, J. Magn. Magn. Matter **100**, 241 (1991).
10. P.H. Dederichs, S. Blügel, R. Zeller, and H. Akai, Phys. Rev. Lett. **53**, 002512 (1984).
11. A. Oswald, R. Zeller, and P. H. Dederichs, J. Magn. Magn. Mater. **54-57**, 1247 (1986); N. Stefanou and N. Papanikolaou, J. Phys.: Condens. Matter **5**, 5663 (1993).
12. A.R. Mackintosh and O.K. Andersen, *The electronic structure of transition metals*, in: *Electrons at the Fermi surface*, Ed. by M. Springfold (Cambridge University Press, Cambridge, 1980); M. Weinert, R. E. Watson, and J. W. Davenport, Phys. Rev. B **32**, 2115 (1985); V. Heine, Solid State Phys. 35, 1 (1980); M. Methfessel and J. Kübler, J. Phys. F 12, 141 (1982).
13. A. Oswald, R. Zeller, P.J. Braspenning, and P.H. Dederichs, J. Phys. F **15**, 193 (1985).
14. L.M. Sandratskii, Phys. Stat. Sol. (b) 135, 167 (1986).
15. S. V. Halilov, H. Eschrig, A. Y. Perlov, and P. M. Oppeneer, Phys. Rev. B **58**, 293 (1998).
16. P. Mavropoulos and N. Papanikolaou, *The Korringa-Kohn-Rostoker (KKR) Green Function Method I. Electronic Structure of Periodic Systems*, in *Computational Nanoscience: Do It Yourself!*, eds. J. Grotendorst, S. Blügel, and D. Marx, Winterschule, 14.-22. Februar 2006, (Forschungszentrum Jülich 2006); `http://www.fz-juelich.de/nic-series/volume31/volume31.html`
17. P.H. Dederichs, S. Lounis, and R. Zeller, *The Korringa-Kohn-Rostoker (KKR) Green Function Method II. Impurities and Clusters in the Bulk and on Surfaces*, in *Computational Nanoscience: Do It Yourself!*, eds. J. Grotendorst, S. Blügel, and D. Marx, Winterschule, 14.-22. Februar 2006, (Forschungszentrum Jülich 2006); `http://www.fz-juelich.de/nic-series/volume31/volume31.html`
18. S. Lounis, Ph. Mavropoulos, P. H. Dederichs, and S. Blügel Phys. Rev. B **72**, 224437 (2005).
19. A.I. Liechtenstein, M.I. Katsnelson, V.P. Antropov, and V.A. Gubanov, J. Magn. Magn. Mater. **67** 65 (1987).
20. P. Bruno, Phys. Rev. Lett. **90**, 087205 (2003).
21. N. Metropolis, A. Rosenbluth, M. Rosenbluth, A. Teller, and E. Teller, J. Chem. Phys. **21**, 1087 (1953).
22. D.P. Landau and K. Binder, *A Guide to Monte Carlo Simulations in Statistical Physics*, Cambridge University Press (2000).

23. S.V. Tyablikov, *Methods of Quantum Theory of Magnetism* (Plenum Press, New York, 1967).
24. H. B. Callen, Phys. Rev. **130**, 890 (1963).
25. M. Pajda, J. Kudrnovsky, I. Turek, V. Drchal, and P. Bruno, Phys. Rev. B **64**, 174402 (2001).
26. E. Sasioglu, L. M. Sandratskii, P. Bruno, and I. Galanakis, Phys. Rev. B **72**, 184415 (2005).
27. See, for example, V.P. Antropov, S.V. Tretyakov, and B.N. Harmon, J. Appl. Phys. **81**, 3961 (1997).
28. V. P. Antropov, M. I. Katsnelson, B. N. Harmon, M. van Schilfgaarde, and D. Kusnezov, Phys. Rev. B **54**, 1019 (1996).
29. L. Greengard and V. Rokhlin, J. Comput. Phys. 73, 325 (1987).
30. Thomas Jourdan, Alain Marty, and Frederic Lancon, Phys. Rev. B **77**, 224428 (2008). A. Desimone, R.V. Kohn, S. Müller, and F. Otto, Multiscale Modeling and Simulation 1, **57** (2003).
31. M. Uhl and J. Kübler, Phys. Rev. Lett. **77**, 334 (1996).
32. J. Kübler, *Theory of Itinerant Electron Magnetism*, Oxford University Press, 2000.
33. A. Gonis, *Theoretical Materials Science*, Materials Science Society, 2000.